Multiple continuous-wave and pulsed modes of a figure-of-eight fibre laser

2013 Laser Phys. 23 035103

(http://iopscience.iop.org/1555-6611/23/3/035103)

Laser Phys. **23** (2013) 035103 (7pp) doi:10.1088/1054-660X/23/3/035103

Multiple continuous-wave and pulsed modes of a figure-of-eight fibre laser

O Pottiez[1], A Martinez-Rios[1], D Monzon-Hernandez[1], G Salceda-Delgado[1], J C Hernandez-Garcia[1], B Ibarra-Escamilla[2] and E A Kuzin[2]

[1] Centro de Investigaciones en Óptica (CIO), Loma del Bosque 115, Colonia Lomas del Campestre, León, Gto. 37150, Mexico
[2] Instituto Nacional de Astrofísica, Óptica y Electrónica (INAOE), L. E. Erro 1, Sta. Ma. Tonantzintla, Pue. 72824, Mexico

E-mail: pottiez@cio.mx

Received 12 September 2012
Accepted for publication 6 November 2012
Published 17 January 2013
Online at stacks.iop.org/LP/23/035103

Abstract
We study experimentally a figure-of-eight fibre laser including a polarization-imbalanced nonlinear optical loop mirror and a Mach–Zehnder optical filter formed by two fibre tapers placed in series. Depending on the adjustments of two wave retarders included in the setup, different modes of operation of the laser are found. In continuous-wave mode, tunable single-wavelength operation as well as multiwavelength lasing are observed. For some adjustments, self-pulsing also takes place, although the pulses are very unstable. Finally, for some adjustments a mechanical stimulation (a kick) leads to the onset of passive mode locking. Measurements reveal that the mode-locked pulses actually are noise-like pulses. Both stable fundamental mode locking and second-harmonic mode locking with particular dynamics were obtained. In this work, we analyse how simple wave plate adjustments can lead to such a variety of operational modes of the fibre laser.

1. Introduction

Fibre lasers are versatile low-cost sources that are attractive for a wide range of applications. In continuous-wave mode, tunable and multiwavelength laser sources are required for wavelength division multiplexing (WDM), fibre sensors and optical instrument calibration, for example [1–7]. On the other hand, self-pulsing, passively Q-switched [8, 9] and mode-locked [10, 11] fibre lasers, operating in pulsed mode, make it possible to reach values of peak power much higher than their continuous-wave counterparts, allowing the use of these sources for studying and exploiting nonlinear effects in fibres, a framework in which supercontinuum generation is now receiving particular attention.

Passively mode-locked figure-of-eight lasers are simple all-fibre sources of ultrashort pulses that are attractive for a wide range of applications [10]. In such devices, the key role of saturable absorber, which is responsible for pulse formation and shortening, is played by a nonlinear optical loop mirror (NOLM) [12], or alternatively by a nonlinear amplifying loop mirror (NALM) [13], which is inserted in the basic fibre ring structure. The nonlinear switching characteristic of a NOLM or NALM are due to the Kerr-induced nonlinear phase difference between the beams that counter-propagate in the loop, and takes the form of a sinusoidal function of input power. An inconvenience of conventional NOLMs, however, is the limited flexibility of the switching characteristic.

In conventional NOLM schemes, switching relies on a power imbalance between the counter-propagating beams, and the polarization dependence of the Kerr effect is not exploited, which limits the adjustment possibilities. An alternative design was proposed, however, in which a polarization difference is induced between the counter-propagating beams [14]. As a 50/50 coupler is used, the device is power symmetric, and polarization asymmetry is created by a quarter-wave retarder (QWR) in the loop. Polarization-dependent nonlinear phase shift (or equivalently nonlinear polarization rotation, NPR) then provides switching. The

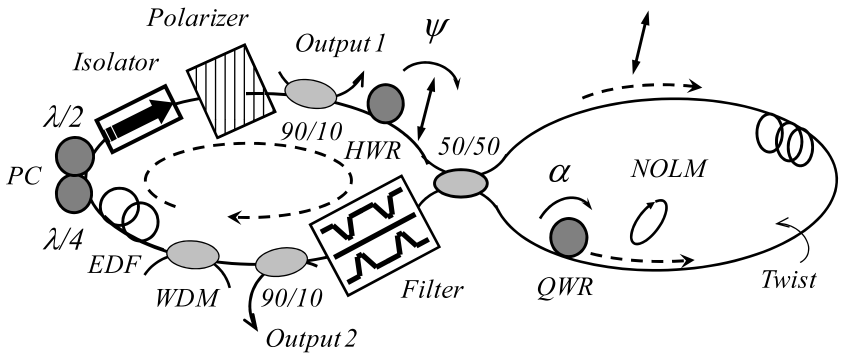

Figure 1. Scheme of the laser under study.

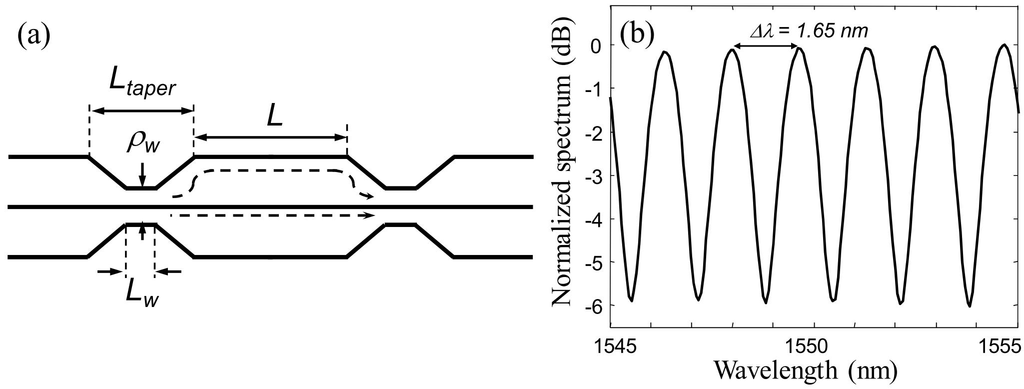

Figure 2. Mach–Zehnder filter formed by two identical fibre tapers in series: (a) schematic design and (b) transmission spectrum in the 1550 nm region. Parameters used for this study: separation between tapers $L = 25$ cm, total taper length $L_{\mathrm{taper}} = 5$ mm, waist diameter $\rho_{\mathrm{w}} = 65$ μm and waist length $L_{\mathrm{w}} = 1$ mm.

fibre is twisted to eliminate random polarization evolution along the loop, and to increase the robustness of the device against environmental perturbations. As the NOLM operation depends on the polarization of light at its input and in the loop, the switching characteristic (in particular, switching power and dynamic range) can be readily adjusted using wave retarders [15, 16]. This polarization-asymmetric scheme was useful for sub-picosecond pulse generation in a figure-of-eight laser [17], and its flexibility allowed setting the conditions of self-starting mode locking operation [18]. By inserting an adjustable bandpass filter in the laser cavity, wavelength-tunable picosecond pulse generation was also demonstrated [19]. Finally, a figure-of-eight laser including a polarization-asymmetric NOLM that generates noise-like pulses was recently developed [20, 21], and these pulses proved to be useful for supercontinuum generation in a piece of standard fibre [22].

In this paper, we propose and study experimentally a figure-of-eight laser scheme including a polarization-imbalanced NOLM as well as a periodic optical filter formed by two fibre tapers in series. Through wave retarder adjustments, several modes of operation of the laser are evidenced in both continuous-wave and pulsed regimes. The experimental results are interpreted in terms of the properties of the NOLM, ring cavity, gain medium and optical filter.

2. Experimental setup

The experimental setup is shown in figure 1. The figure-of-eight laser is formed by a ring laser cavity (left side of the figure) in which a polarization-imbalanced NOLM is inserted (right). The ring cavity includes a 4 m long erbium-doped fibre (EDF) with 30 dB m^{-1} absorption at 1530 nm, which is pumped by a 980 nm laser diode through a WDM coupler. The maximum pump power into the fibre is ∼300 mW. A polarizer ensures linear polarization at the NOLM input, whose angle ψ can be adjusted by a half-wave retarder (HWR). A polarization controller (PC) made of two retarder plates is used to maximize the power through the polarizer. An optical isolator ensures unidirectional laser operation. Two output couplers (10% output coupling) provide the laser output ports. The ring also includes an optical filter, which consists of two concatenated fused fibre tapers (figure 2(a)). The filter was fabricated in a Nufern 980HP fibre using a Vytran glass processor. This device is a Mach–Zehnder interferometer: at the first taper the fundamental core mode partially couples to cladding modes and a fraction of the light guided in the cladding couples back to the core at the second taper [23]. The transmission spectrum of the filter is thus a periodic pattern resulting from the interference between core and cladding modes of the fibre (figure 2(b)). For the device dimensions used in this work and given in

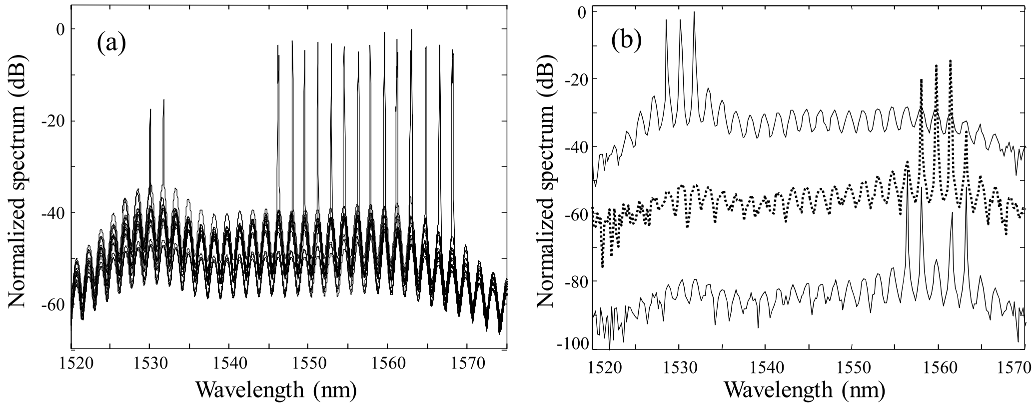

Figure 3. Optical spectra in the continuous-wave regime: (a) tunable single-wavelength operation and (b) multiple-wavelength operation (spectra are shifted for better readability).

figure 2, the interference pattern presents a period of 1.65 nm, a modulation depth of ∼6 dB and an insertion loss of ∼0.5 dB. It has to be noted that no bending was applied to the filter.

The NOLM is formed by a 50/50 coupler and a 100 m loop of low birefringence, highly twisted (5 turns m^{-1}) Corning SMF-28 fibre. A QWR is inserted to break the polarization symmetry: whereas the clockwise beam remains linearly polarized in the loop, the polarization of the counter-clockwise beam is made elliptic by the QWR, the value of ellipticity depending on the angle ψ of input polarization with respect to the QWR. The fibre loop has an anomalous dispersion of ∼17 ps nm^{-1} km^{-1} and a nonlinear coefficient $\gamma = 1.5$ W^{-1} km^{-1} for linearly polarized light ($\beta = 2/3\gamma = 1$ W^{-1} km^{-1} for circular polarization). With these parameters, the minimum continuous-wave switching power of the NOLM is $P_\pi = 4\pi/\beta L \approx 125$ W [15]. Controlling the linear input polarization angle ψ and QWR angle α allows adjustment of the NOLM switching power and dynamic range, respectively [15, 16].

3. Results and discussion

3.1. Continuous-wave operation

At maximal pump power, for most positions of the wave retarders, continuous-wave operation is obtained in the 1550 nm region. As expected, the highest output power is observed at output 1, reaching ∼4 mW. Adjustments of the QWR and HWR allow tuning single-wavelength laser oscillation over more than 20 nm, between 1546 and 1568 nm, in steps of 1.65 nm, corresponding to the filter spectral period (figure 3(a)). Single-wavelength operation in the 1530 nm region was also observed. In contrast, lasing in the 1540 nm region could not be observed due to a slight dip in the gain spectrum (visible in the spontaneous emission spectra of figure 3). The use of a gain flattening technique (e.g. a long-period grating, or a second, shorter Mach–Zehnder filter) would thus be required to improve the tunability range. Wavelength tunability is due to two mechanisms. First, considering that the QWR angle allows adjustment of the NOLM low-power transmission, it turns out that the NOLM works at low power as a tunable attenuator, whose attenuation can be adjusted by the QWR [15]. By adjusting the laser intracavity loss in this way one modifies the balance between absorption and emission that determines the gain spectrum of the EDF [24], and thus the position of the gain maximum where lasing will take place. Secondly, the residual birefringence present in the cavity and the polarizer are responsible for a coarse filtering effect or wavelength-dependent loss, which can be adjusted through the wave plates and also contributes to the selection of the operating wavelength [25].

For proper adjustments of the QWR and HWR, multiple-wavelength continuous-wave operation was also observed (figure 3(b)). Although simultaneous lasing at closely spaced wavelengths in homogeneously broadened media is challenging due to competition between lines, we were able to observe up to three-wavelength operation in the 1530 and 1550 nm regions, with a wavelength spacing of 1.65 nm in both cases. A fourth wavelength sometimes appears transitorily; however, its intensity is substantially smaller. Two sets of two closely spaced wavelengths separated by 3.3 nm (two filter periods) were also observed in the 1550 nm region. In order to maintain simultaneous lasing of contiguous lines in spite of severe competition, precise gain/loss adjustments at different wavelengths are required [4–7]. In this case, this was performed through wave plate adjustments, using the same mechanisms as those described previously for wavelength tuning. Stable multiwavelength operation was not maintained beyond a few minutes, however, unless readjustments of the wave plates were performed.

3.2. Mode locking

For particular positions of the HWR and QWR, a mechanical stimulation (a kick) results in the onset of the mode locking operation, which is evidenced by the wide optical spectrum of bandwidth several tens of nanometres, and by the observation on a 200 MHz oscilloscope of a periodic pulse train. The pulse train repetition rate is ∼1.6 MHz (period = 600 ns), indicating fundamental frequency mode

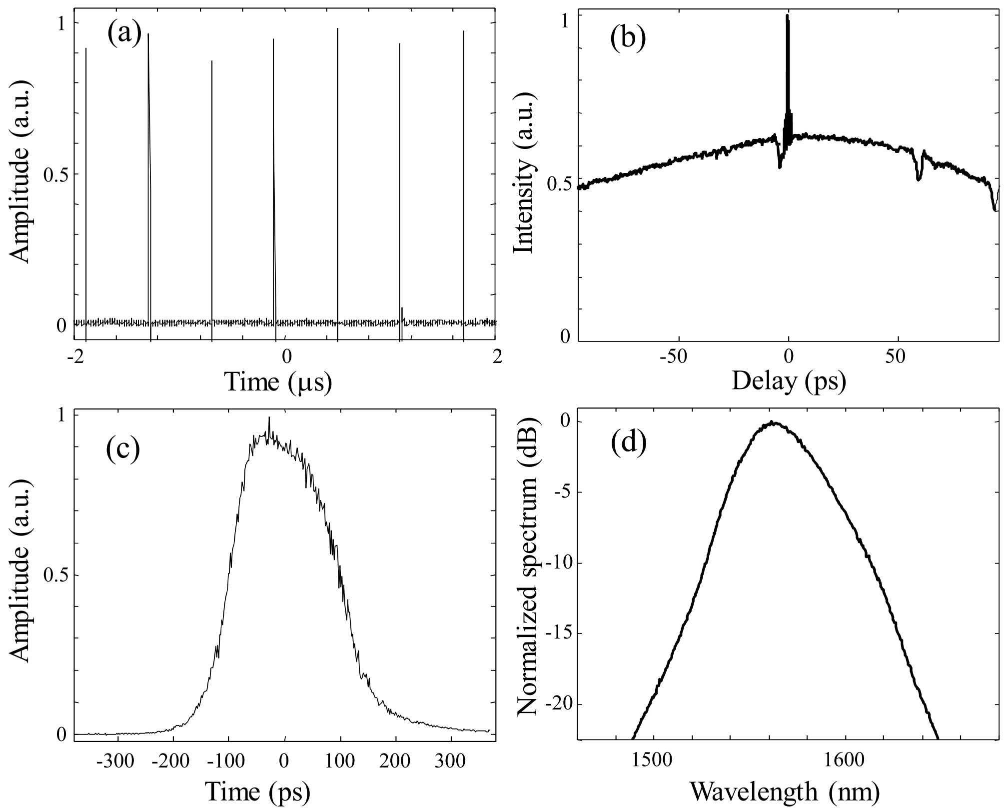

Figure 4. Measurements in the fundamental mode locking regime: (a) pulse train observed with a 2 GHz photodetector and a 200 Mz oscilloscope; (b) optical autocorrelation; (c) single pulse observed with a 25 GHz photodetector and a sampling scope; (d) optical spectrum.

locking of the ~120 m long laser cavity (figure 4(a)). A closer analysis reveals that the pulses actually are noise-like pulses. Noise-like pulses are large collections of ultrashort pulses with randomly varying amplitudes and durations, which were observed and studied in a number of previous works [20, 21, 26–33], and whose properties are particularly attractive for supercontinuum generation [22, 34]. Once mode locking is obtained for given wave plate adjustments, it is maintained within a narrow range of variation of the HWR angle (about 10°) about its initial position, although the pulses' temporal and spectral properties vary within this range. If the HWR is rotated beyond this range, mode locking is lost and the laser returns to the continuous-wave regime. Figure 4(b) shows a typical optical autocorrelation of the pulses. It presents a double-scale structure that is typical of noise-like pulses, with a narrow sub-picosecond (~150 fs) peak riding a wide pedestal that extends beyond the 200 ps measurement window of the autocorrelator. The central spike scales as the duration of the sub-pulses in the bunch, whereas the pedestal extension is related to the total duration of the noise-like pulse. The duration of the bunch was measured directly using a fast (25 GHz) photodetector and a 50 GHz bandwidth sampling oscilloscope, yielding a value of ~200 ps (figure 4(c)). Finally, figure 4(d) presents the optical spectrum measured at output 1 using an optical spectrum analyser. The spectrum is very wide (~40 nm at half maximum), which is a common feature of noise-like pulses. It is noteworthy that, contrary to the continuous-wave case, the spectral modulation introduced by the filter is not visible in figure 4(d). The spectrum is slightly asymmetric as a consequence of intracavity Raman self-frequency shift, which transfers energy from the short wavelength side of the spectrum to longer wavelengths.

The results presented here in the fundamental mode locking regime are similar to those obtained previously for the figure-of-eight laser without a filter, which was the same setup as figure 1 but excluding the Mach–Zehnder filter [20, 21]. This leads to the conclusion that the periodic filter has little influence on this mode of operation of the laser. Mode locking is observed only for particular positions of the QWR, which correspond to small (although non-zero) low-power transmission of the NOLM, and which ensure that the NOLM operates as a saturable absorber (i.e. transmission grows with increasing input power) and not as an intensity limiter (transmission decreases with power). Proper adjustment of the HWR is also essential for mode locking operation, as it allows control of the NOLM switching power. As this power corresponds to maximal transmission through the NOLM, the pulse peak power tends to adjust itself to this value. If the switching power is too high, however, it may be unreachable for given pump power conditions, yielding too small pulse transmission through the NOLM (i.e. not significantly above low-power transmission), and mode locking is not observed in such cases. Of course, this simple picture is complicated in the case of noise-like pulses, which are collections of sub-pulses with different amplitudes that cannot match simultaneously a given value of the switching power. However, it is conceivable that, even in this case, the transmission of the bunch through the NOLM will depend on the value of switching power,

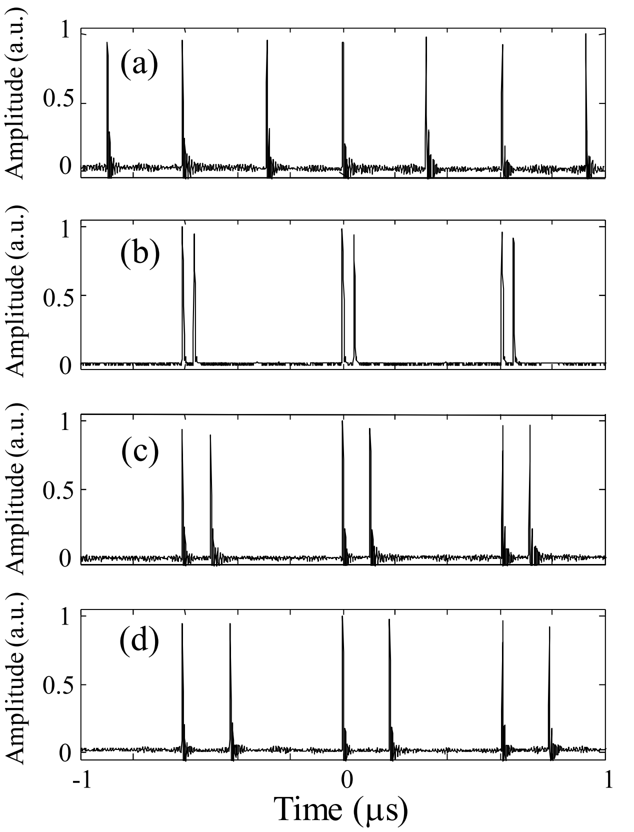

Figure 5. Second-harmonic mode-locked pulse train observed with a 2 GHz photodetector and a 200 Mz oscilloscope, at different times.

in particular it will be small (comparable with low-power transmission) if switching power is too large compared to the amplitude of the highest pulses in the bunch, so that again mode locking will be observed only for certain adjustments of the HWR. In summary, proper adjustments of the NOLM nonlinear characteristic through the QWR and HWR are required for mode locking operation.

Contrary to the laser without a filter [20, 21], for which only fundamental mode locking was observed, second-harmonic mode locking was also observed with the setup of figure 1. Indeed, for particular positions of the wave retarders, not one but two noise-like pulses appear in the cavity (figure 5). During most of the time, a stable train of uniformly spaced pulses with a period of ∼300 ns is observed on the scope (figure 5(a)); however, typically after a few seconds the second pulse disappears from its central position and re-emerges immediately from the first pulse, then moves away from it back to its initial central position where it stabilizes again for a few seconds (figures 5(b)–(d)). This walkoff (from pulse splitting to the uniform distribution of pulses) lasts for about 1 s. The optical spectrum and autocorrelation trace obtained in this regime are similar to those of figures 4(b) and (d) for fundamental mode locking. A regime of coexistence of two noise-like pulses in a fibre laser was already observed previously [27]; however, in the present case no splitting of the spectrum was observed.

Although the mechanism of this second-harmonic mode locking of noise-like pulses is not completely understood, some elements of response can be found in the literature [35]. As shown in that work, the behaviour of solitons in a bunch depends on the interaction between these solitons and their nonsoliton components (dispersive waves). These interactions cause small shifts of the central soliton wavelength, whose sign and strength depend on the phase between solitons and dispersive waves. For certain phase adjustments, these shifts cause a repulsive interaction in the dispersive fibre between solitons. As the phase between solitons and nonsoliton components can be controlled through wave retarders, particular adjustments may create the conditions for a repulsive interaction between two subsets of pulses in the bunch, which therefore splits in two. By considering the walkoff speed observed experimentally and the value of anomalous dispersion of the fibre, one can estimate that the wavelength shift is very small, of the order of 0.1 nm. Once the separation between the two groups of pulses reaches half the cavity round-trip time, walkoff stops and the pulses remain locked into their temporal positions (at least for a few seconds). This temporary stabilization of the pulses may be related to acoustic effects [35]. Another relevant aspect of the setup of figure 1 is the presence of the Mach–Zehnder filter, which at each pass delays the two fractions of the signal before recombining them. Considering the spectral period of 1.65 nm of the filter, one can estimate that this delay amounts to ∼5 ps per pass through the filter. Although this value is much smaller than the total duration of the noise-like pulse, it is significantly larger than the average duration of the inner sub-pulses (∼100 fs according to the autocorrelation measurement), so that it may still favour bunch splitting. It has to be stressed, however, that this 5 ps delay per round trip caused by the filter cannot be responsible for the observed walkoff, as one can calculate that this value yields a much shorter walkoff duration (∼36 ms) than experimentally observed (∼1 s).

3.3. Self-pulsing

Finally, a regime of self-pulsing was also observed for some adjustments of the retarders. As shown in figure 6(a), the laser behaviour varies considerably, producing a train of pulses that in some instances reduces to a mere sinusoidal waveform. Although highly variable, the period and duration of the pulses are of the order of 50 μs and 10 μs, respectively. Figure 6(b) shows a close-up of one pulse, showing amplitude modulation at the cavity fundamental frequency and its 12th harmonic, due to the beat note between resonant cavity modes. The optical spectrum (figure 6(c)) is also highly variable in time, and usually includes many spectral components, although one of them is at least 15–20 dB higher than the others.

Whereas passive mode locking requires a fast saturable absorber action (here provided by the NOLM), self-pulsing is obtained with a slow saturable absorber. In this case the saturable absorber action that yields self-pulsing is likely to originate from erbium clusters (or pairs) in the highly doped erbium fibre [36]. The tendency of the laser to operate spontaneously in continuous-wave or self-pulsing mode depends on several parameters, in particular the intracavity loss (photon lifetime) [8]. In the present case, wave retarders

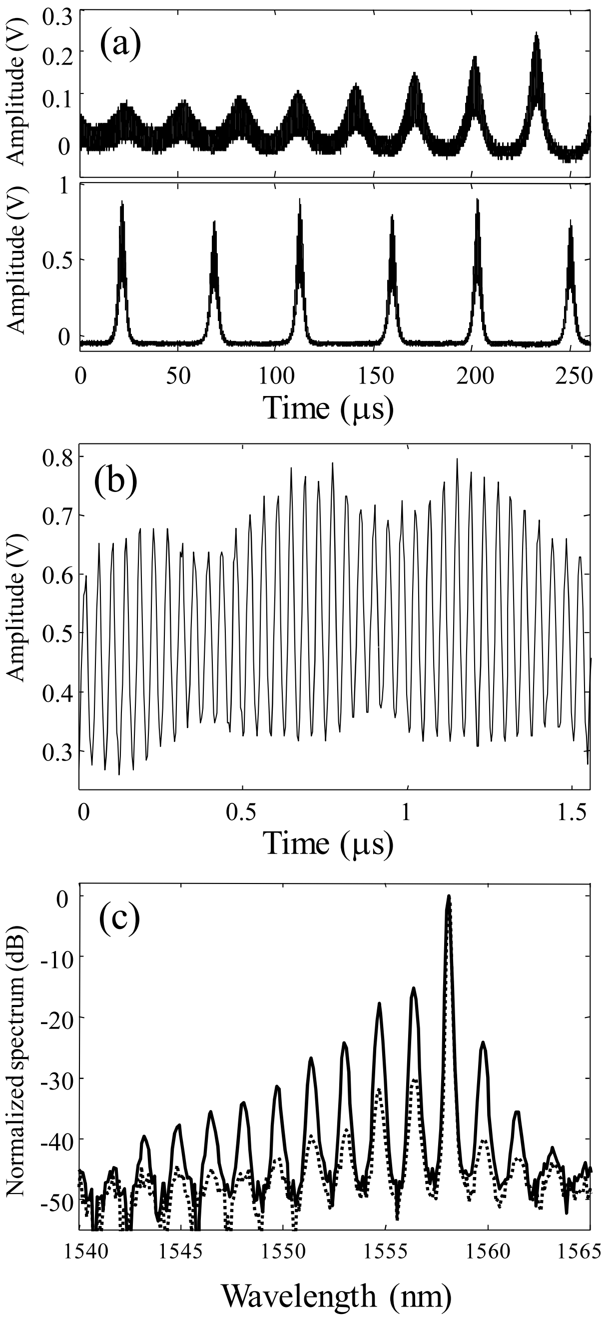

Figure 6. (a) Scope traces of the self-pulsing signal at two different times; (b) detail of a single pulse; (c) optical spectrum at two different times.

allow adjustment of the intracavity loss; in particular, as already mentioned, the Sagnac interferometer including a rotatable QWR operates like a tunable attenuator. In the presence of erbium ion pairs, self-pulsing tends to prevail when the wave retarders are adjusted for large intracavity loss (short photon lifetime). The poor stability of the self-pulsing regime in this study may be related to a low proportion of erbium pairs in the total erbium population.

4. Conclusions

In this work, we performed an experimental study of an erbium-doped figure-of-eight fibre laser including a polarization-imbalanced NOLM and a Mach–Zehnder optical filter formed by two concatenated fibre tapers. Light polarization is controlled by a QWR in the NOLM and by a HWR in the ring section of the laser, which also includes a polarizer. This polarization control allows adjustment of the transmission properties of the NOLM and ring cavity, which in turn allows establishment of the specific conditions under which different operational modes of the laser appear. The filter, by defining periodic windows in the spectrum and by introducing a delay at each round trip, also plays a key role in most modes of operation. In the continuous-wave regime, single-wavelength operation is observed with a tunability range that extends over more than 20 nm in steps of 1.65 nm, which corresponds to the spectral period of the filter. Simultaneous continuous-wave lasing at up to three wavelengths separated by 1.65 nm is also demonstrated. Non-self-starting mode locking is also observed, in the form of generation of noise-like pulses. Both fundamental and second-harmonic mode locking are also obtained, with in the latter case the onset of a transient walkoff between the two pulses. Finally, an unstable self-pulsing behaviour is also evidenced. This work demonstrates that polarization control in a fibre laser together with wavelength selection can give access to a wide variety of modes of operation that are useful for applications in the frame of optical transmission, sensing or supercontinuum generation, among others.

Acknowledgments

O Pottiez was supported by CONACyT grant 130681. G Salceda-Delgado acknowledges also to CONACYT for a PhD fellowship.

References

[1] Liu Y, Dong X, Shum P, Yuan S, Kai G and Dong X 2006 *Opt. Express* **14** 9293–8
[2] Chen D, Qin S and He S 2007 *Opt. Express* **15** 930–5
[3] Xiu-jie J, Yan-ge L, Li-bin S, Zhan-cheng G, Sheng-gui F, Gui-yun K and Xiao-yi D 2008 *Opt. Commun.* **281** 90–3
[4] Durán-Sánchez M, Flores-Rosas A, Álvarez-Tamayo R I, Kuzin E A, Pottiez O, Bello-Jimenez M and Ibarra-Escamilla B 2010 *Laser Phys.* **20** 1270–3
[5] Al-Alimi A W, Al-Mansoori M H, Abas A F, Mahdi M A, Ajiya M and MahamdAdikan F R 2010 *Laser Phys.* **20** 2001–5
[6] Latif A A, Zulkifli M Z, Awang N A, Harun S W and Ahmad H 2010 *Laser Phys.* **20** 2006–10
[7] Yeh C H, Chow C W, Wu Y F, Lin Y H, Cheng B C and Chen J H 2011 *Laser Phys. Lett.* **8** 672–7
[8] Sanchez F, Le Boudec P, François P-L and Stephan G 1993 *Phys. Rev.* A **48** 2220–9
[9] Kurkov A S, Sadovnikova Y E, Marakulin A V and Sholokhov E M 2010 *Laser Phys. Lett.* **7** 795–7
[10] Duling I N III 1991 *Opt. Lett.* **16** 539–41
[11] Matsas V J, Richardson D J, Newson T P and Payne D N 1993 *Opt. Lett.* **18** 358–60
[12] Doran N J and Wood D 1988 *Opt. Lett.* **13** 56–8
[13] Fermann M E, Haberl F and Hofer M 1990 *Opt. Lett.* **15** 752–4
[14] Kuzin E A, Korneev N, Haus J W and Ibarra-Escamilla B 2001 *J. Opt. Soc. Am.* B **18** 919–25

[15] Pottiez O, Kuzin E A, Ibarra-Escamilla B and Mendez-Martinez F 2005 *Opt. Commun.* **254** 152–67
[16] Ibarra-Escamilla B, Kuzin E A, Zaca-Moran P, Grajales-Coutiño R, Mendez-Martinez F, Pottiez O, Rojas-Laguna R and Haus J W 2005 *Opt. Express* **13** 10760–7
[17] Kuzin E A, Ibarra-Escamilla B, Garcia-Gomez D E and Haus J W 2001 *Opt. Lett.* **26** 1559–61
[18] Ibarra-Escamilla B, Pottiez O, Kuzin E A, Haus J W, Grajales-Coutiño R and Zaca-Moran P 2008 *Opt. Commun.* **281** 1226–32
[19] Ibarra-Escamilla B, Pottiez O, Haus J W, Kuzin E A, Bello-Jimenez M and Flores-Rosas A 2008 *J. Eur. Opt. Soc.* **3** 08036
[20] Hernandez-Garcia J C, Pottiez O, Grajales-Coutiño R, Ibarra-Escamilla B, Kuzin E A, Estudillo-Ayala J M and Gutierrez-Gutierrez J 2011 *Laser Phys.* **21** 1518–24
[21] Pottiez O, Grajales-Coutiño R, Ibarra Escamilla B, Kuzin E A and Hernandez-Garcia J C 2011 *Appl. Opt.* **50** E24–31
[22] Hernandez-Garcia J C, Pottiez O and Estudillo-Ayala J M 2012 *Laser Phys.* **22** 221–6
[23] Monzon-Hernandez D, Martinez-Rios A, Torres-Gomez I and Salceda-Delgado G 2011 *Opt. Lett.* **36** 4380–2
[24] Franco P, Midrio M, Tozzato A, Romagnoli M and Fontana F 1994 *J. Opt. Soc. Am.* B **11** 1090–7
[25] Gonzalez-Garcia A, Pottiez O, Ibarra-Escamilla B and Kuzin E A 2010 *Laser Phys.* **20** 720–5
[26] Horowitz M, Barad Y and Silberberg Y 1997 *Opt. Lett.* **22** 799–801
[27] Horowitz M and Silberberg Y 1998 *IEEE Photon. Technol. Lett.* **10** 1389–91
[28] Kang J U 2000 *Opt. Commun.* **182** 433–6
[29] Tang D Y, Zhao L M and Zhao B 2005 *Opt. Express* **13** 2289–94
[30] Zhao L M and Tang D Y 2006 *Appl. Phys.* B **83** 553–7
[31] Zhao L M, Tang D Y and Wu J 2007 *Opt. Express* **15** 2145–50
[32] Kobtsev S, Kukarin S, Smirnov S, Turitsyn S and Latkin A 2009 *Opt. Express* **17** 20707–13
[33] Vazquez-Zuniga L A and Jeong Y 2012 *IEEE Photon. Technol. Lett.* **24** 1549–51
[34] Takushima Y, Yasunaka K, Ozeki Y and Kikuchi K 2005 *Electron. Lett.* **41** 399–400
[35] Grudinin A B and Gray S 1997 *J. Opt. Soc. Am.* B **14** 144–54
[36] Colin S, Contesse E, Le Boudec P, Stephan G and Sanchez F 1996 *Opt. Lett.* **21** 1989